AD-A130 789 SINGLE CRYSTAL ALLOY FILM INFRARED DETECTORS(U) ITT 1/1
ELECTRO-OPTICAL PRODUCTS DIV ROANOKE VA A AMITH ET AL.
OCT 81 N60921-80-C-0105

UNCLASSIFIED F/G 20/12 NL

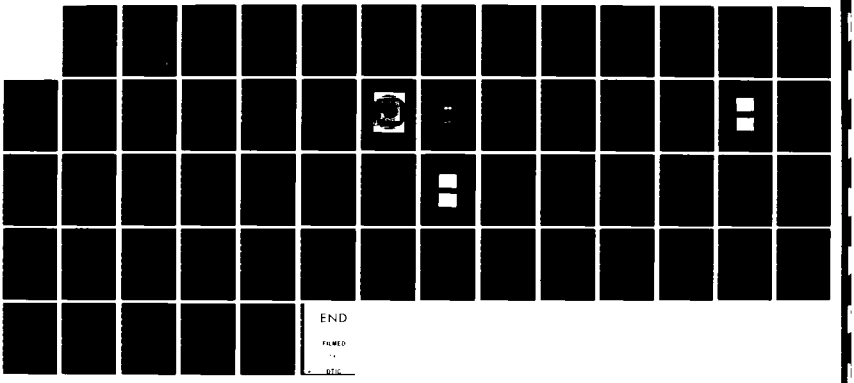

END

FILMED

DTIC

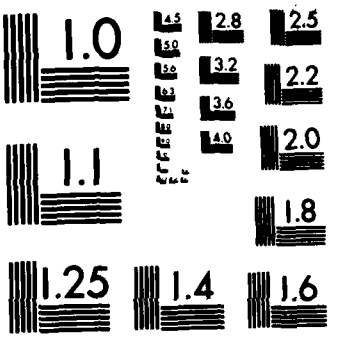

SINGLE CRYSTAL ALLOY FILM INFRARED DETECTORS

FINAL TECHNICAL REPORT

For Period July 21, 1980-July 21, 1981

Contract N60921-80-C-0105

ITT Project 35007

ELECTRO-OPTICAL PRODUCTS DIVISION ITT

SINGLE CRYSTAL ALLOY FILM

INFRARED DETECTORS

FINAL TECHNICAL REPORT

For Period July 21, 1980-July 21, 1981

Contract N60921-80-C-0105

ITT Project 35007

Prepared for:

Naval Surface Weapons Center
White Oak
Silver Spring, Maryland 20910

Prepared by:

ITT Electro-Optical Products Division
7635 Plantation Road, N.W.
Roanoke, Virginia 24019

Approved by:

A. Amith 3/12/82

A. Amith, Manager,
Electro-Optical Devices Group

Date: March 12, 1982
Doc Id No: 81-39-07

UNCLASSIFIED

SECURITY CLASSIFICATION OF THIS PAGE (When Data Entered)

REPORT DOCUMENTATION PAGE	READ INSTRUCTIONS BEFORE COMPLETING FORM
1. REPORT NUMBER	2. GOVT ACCESSION NO. AD-A130789	3. RECIPIENT'S CATALOG NUMBER
4. TITLE (and Subtitle) SINGLE CRYSTAL ALLOY FILM INFRARED DETECTORS	5. TYPE OF REPORT & PERIOD COVERED Final Technical Report July 21, 1980-July 21, 1981
	6. PERFORMING ORG. REPORT NUMBER
7. AUTHOR(s) A. Amith M. Drinkwine J. Rozenbergs	8. CONTRACT OR GRANT NUMBER(s) N60921-80-C-0105
9. PERFORMING ORGANIZATION NAME AND ADDRESS ITT Electro-Optical Products Divison 7635 Plantation Road, N.W. Roanoke, Virginia 24019	10. PROGRAM ELEMENT, PROJECT, TASK AREA & WORK UNIT NUMBERS NIF;0;0;0R45JC
11. CONTROLLING OFFICE NAME AND ADDRESS Naval Surface Weapons Center White Oak, Silver Spring, MD 20910 Attn: Code R45	12. REPORT DATE October 1981
	13. NUMBER OF PAGES 50
14. MONITORING AGENCY NAME & ADDRESS(if different from Controlling Office)	15. SECURITY CLASS. (of this report) UNCLASSIFIED
	15a. DECLASSIFICATION/DOWNGRADING SCHEDULE

16. DISTRIBUTION STATEMENT (of this Report)
Approved for public release: distribution unlimited.

17. DISTRIBUTION STATEMENT (of the abstract entered in Block 20, if different from Report)

18. SUPPLEMENTARY NOTES

19. KEY WORDS (Continue on reverse side if necessary and identify by block number)

20. ABSTRACT (Continue on reverse side if necessary and identify by block number)
Activation techniques have been developed to produce enhanced performance and increased yield of $PbS_{0.5}Se_{0.5}$ detectors with large area (3.2×10^{-2} cm^{-2}) for detection of infrared (ir) radiation in the 3 μm to 5 μm band. Incorporation of chloride at the Pb salt surface and/or heat treatment annealing of the detector have been effective in enhancing device performance. The heat treatment technique which produces a diffused Pb salt/Pb interface has given

DD FORM 1 JAN 73 1473 EDITION OF 1 NOV 65 IS OBSOLETE

UNCLASSIFIED

SECURITY CLASSIFICATION OF THIS PAGE (When Data Entered)

20. ABSTRACT (continued)

the best results in terms of performance and yield. These results do not preclude the necessity of obtaining high quality epitaxial Pb salt thin films as the basis for detector fabrication (i.e., $\mu_H \simeq 10{,}000$ cm^2 V^{-1} s^{-1} at 77 K and $p \simeq 1\text{-}3 \times 10^{17}$ cm^{-3}).

PREFACE

The purpose of this contract was to achieve a more thorough understanding of the fabrication technology of IV-VI semiconductor Schottky barrier detectors. Using the technology developed by the Naval Surface Weapons Center (NSWC) at White Oak, Pb Schottky contacts were deposited on epitaxial $PbS_{0.5}Se_{0.5}$ using various methods of fabrication to enhance the detector performance.

The work reported here was supported by the Department of the Navy, NSWC, White Oak, Maryland, under contract N60921-80-C-0105.

The work was carried out at ITT Electro-Optical Products Division (EOPD), Roanoke, Virginia. Major contributions to this work were made by A. Amith, M. J. Drinkwine, J. Rozenbergs, and S. R. Jost. Assistance was also provided by S. B. Phatak, W. D. Mims, and J. S. Wei.

TABLE OF CONTENTS

LIST OF ILLUSTRATIONS (continued)

1.0 INTRODUCTION

Previous work at NSWC, White Oak,[1] and elsewhere[2] demonstrated the feasibility of obtaining high performance IV-VI metal-semiconductor photovoltaic detectors. However, these devices, made by depositing a Pb Schottky contact onto epitaxially grown PbSSe films on BaF_2 substrates, could not be produced with consistently good results. A number of good and bad diodes were obtained from NSWC and analyzed by Auger electron spectroscopy at ITT EOPD. These measurements revealed the presence of unintentionally introduced chlorine at the Pb/PbSSe interface of good diodes (see Figure 1.0-1) and an absence of this material in devices having poor diode characteristics. Following these preliminary results, a program was initiated to investigate the effectiveness of a chloride or oxychloride enriched interface in producing enhanced performance of Pb/$PbS_{0.5}Se_{0.5}$ photodiodes.

This is the final report of this program to investigate the interfacial factors which affect the electrical and optical properties of the metal-semiconductor contact between Pb and p-type $PbS_{0.5}Se_{0.5}$ and produce IV-VI Schottky barrier detector fabrication techniques which will pave the way for device production.

The report contains a summary of the program's results. The preparation and growth of the epitaxial films is presented in

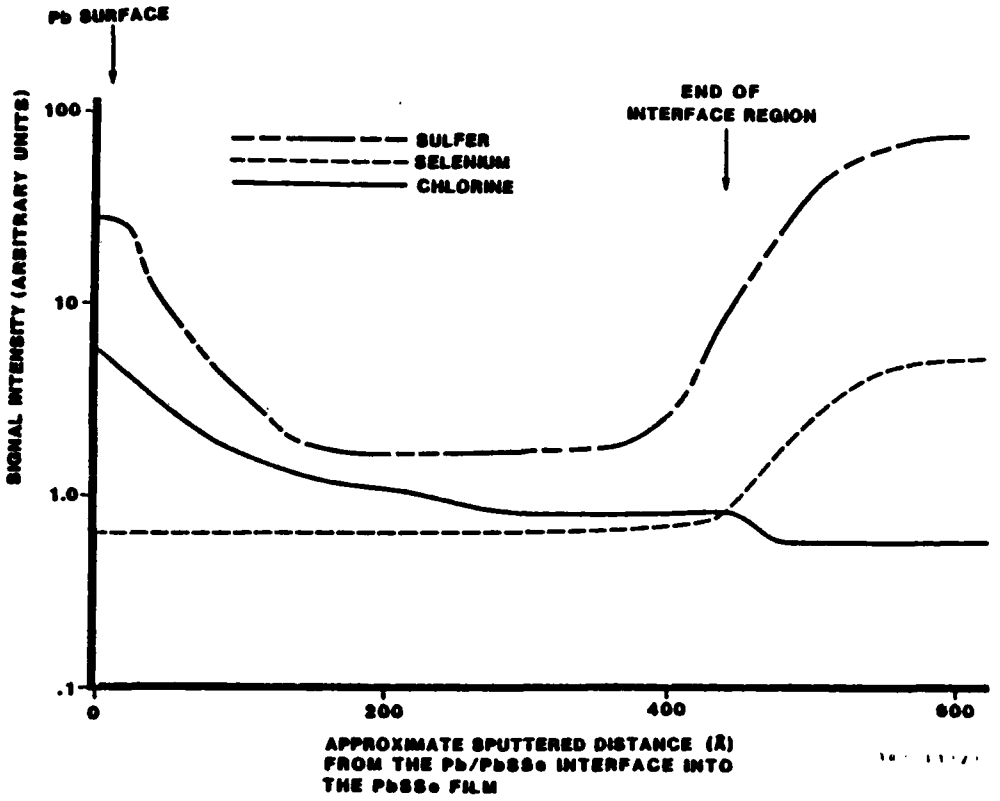

Figure 1.0-1. Sputter Profile of PbSSe Under the Pb Contact of a Good Schottky Diode.

Section 2.0. Section 3.0 describes the device fabrication procedure, and device sensitization techniques are presented in Section 4.0. Section 5.0 discusses device characterization measurements. In Section 6.0 the results are interpreted in terms of the Schottky, MIS, and pn junction models of the sensitized metal-semiconductor interface. Finally, in Section 7.0, conclusions and recommendations are presented.

2.0 MATERIAL GROWTH

Methods of growing thin epitaxial lead salt films by vacuum deposition have been described by many authors.[3] [4] [5] The particular technique used in ITT EOPD's work is a simplified version of the technique used by Holloway.[6]

Lead salt source material was prepared by alloying high purity lead, sulfur, and selenium in an evacuated sealed quartz ampul at +1130°C for 24 h or longer. Initial combination of the sulfur with the lead posed a safety hazard because of the rapid increase in the sulfur vapor pressure with temperature. A careful cyclic heating with a torch was required to react the sulfur with the lead and prevent an explosive buildup of high pressure within the quartz ampul. After the initial combination of the lead, sulfur, and selenium, the alloying was performed using a tube furnace. PbS and $PbS_{0.5}Se_{0.5}$ were produced by this method.

X-ray (energy dispersive) analysis was performed on the lead salt source material. Results indicated that unknown contaminants (confirmed as oxygen by Auger electron spectroscopy) were present in large quantities in pieces of source material which had a blackish, coal-like appearance. Shiny metallic-like pieces of source material were devoid of significant quantities of contaminants. Care was taken not to use pieces of source material having a coal-like appearance for a deposition of epitaxial lead salt

films. In some cases the alloyed lead salt material was pulverized and realloyed using only the metallic pieces from the first alloy to form the second alloy. No obvious difference was observed comparing the second alloy to the first. There was also no obvious difference in the quality of the lead salt films obtained from first alloy source material versus second alloy source material. (However, it should be noted that unavoidable variances in the thin film growth process in this work play a stronger role than the variances in source material in determining the quality of the grown film.) The highest quality source material was obtained by performing extended evacuation of the quartz ampul prior to sealing and alloying for more than 72 h.

Source material was loaded into a baffled tantalum evaporation boat of the type used for thermal deposition of silicon monoxide. The boat was placed in a commercial diffusion pumped evaporation system (Veeco model 300) and connected to high current (200 A capacity) feedthroughs. Sulfur and selenium were loaded into a small quartz tube closed on one end and restricted to a narrow aperture at the other end. This tube provided an auxiliary source of sulfur/selenium during the evaporation; this excess chalcogenide is necessary to produce p-type lead salt epitaxial films. The tube was placed on the base plate of the evaporator with the aperture aimed toward the substrate heater and heat shielded by a metal sheet between it and the source boat. The temperature of

the auxiliary source proved to be a crucial parameter which remained poorly controlled with this setup. This was a major source of problems adversely affecting the quality of the lead salt films grown in this study.

Single crystal barium fluoride crystals were used as the substrate on which the lead salt thin films were grown/evaporated. The BaF_2 substrates were freshly cleaved to a thickness of about 0.5 mm to 1.0 mm and mounted onto the substrate heater prior to each growth run. BaF_2 substrates nearly free of all cleavage steps were obtained by cleaving cooled crystals (however, this improved technique was not employed until close to the end of this study).

The substrate heater was suspended above the evaporation source at a distance of ~20 cm-25 cm. Temperature uniformity across the substrate heater proved a necessary requirement for achieving uniformly heated substrates and high quality lead salt films. A graphite block heated by tantalum heater wires insulated by means of ceramic tubes passing through the block was found to provide sufficient temperature uniformity to uniformly heat four 1/2-in square BaF_2 substrates, mounted side by side, during a growth run.

A chromel-alumel thermocouple was mounted inside the heater block near the center for temperature measurement to provide for temperature control during the growth/evaporation process. A quartz

crystal oscillator was suspended next to the substrate heater to provide a means of monitoring the rate of deposition during the growth run. A mechanical shutter was positioned between the evaporation source and the BaF_2 substrates to prevent deposition of lead salts until outgassing of the source material had been completed.

It was found that components in the system composed of copper or nickel decomposed rapidly because of the corrosive action of sulfur vapor in contact with these metals. Substitution of aluminum for copper as an electrical conductor proved an effective solution to this problem. In cases where a direct substitution was impossible, it was found that gold plating of the copper provided effective protection against the corrosive effects of the sulfur.

A base pressure of $\sim 10^{-6}$ torr was routinely achieved with the vacuum system used for growth of the lead salt epitaxial films. Heating of the substrate heater was initiated upon reaching the base pressure of $\sim 10^{-6}$ torr. The substrate heater temperature was raised to >+400°C for 30-60 min for outgassing of the heater and substrates prior to deposition. After thorough outgassing, the substrate heater temperature was lowered to the growth temperature of between +350°C and +400°C. The lead salt source boat was then heated slowly until evaporation was indicated on the quartz crystal monitor. The deposition rate was adjusted to between

5 and 15 Å/s. Approximately 0.5 μm of material was deposited to thoroughly outgas the source before opening the shutter and exposing the BaF_2 substrates. The shutter was then opened and deposition of lead salt material on the heated BaF_2 substrates proceeded at a constant rate of <15 Å/s until ~2.5 μm had been deposited on the substrates. The shutter was then closed and the substrate heater and source turned off. System pressure during growth/evaporation rose typically to the low 10^{-5} torr range.

As mentioned, the temperature of the auxiliary chalcogenide source played a crucial role in determining the quality of the epitaxial lead salt films. With the system used here it was finallly determined impossible to achieve the control necessary for consistent results. Only several of the numerous films grown had the desired properties of high Hall mobility and moderate p-type carrier concentration (i.e., ~10^{17} cm^{-3}). Use of sulfur alone in the auxiliary source proved suitable for growth of PbS films but not for $PbS_{0.5}Se_{0.5}$ films. Unless selenium was placed in the auxiliary source along with sulfur, attempts to grow $PbS_{0.5}Se_{0.5}$ films resulted in very high carrier concentration p-type films of composition $PbS_{1-x}Se_x$ with x as small as ~0.2. Theoretically, sulfur alone in the auxiliary source should be capable of producing moderate carrier concentration p-type $PbS_{0.5}Se_{0.5}$ films using $PbS_{0.5}Se_{0.5}$ source material because only a slight overpressure

of chalcogenide is required to prevent n-type films from forming. However, the high temperatures at the auxiliary source in ITT EOPD's system produce extreme overpressures of sulfur giving the growth results observed here. It was found that the presence of selenium in the auxiliary source had a moderating effect on the rate of sulfur evaporation from the auxiliary source as well as providing an overpressure of both S and Se to maintain films of composition close to that of the source material (i.e., $PbS_{0.5}Se_{0.5}$).

The present conclusion concerning use of the auxiliary chalcogenide source is that due to lack of adequate control of the temperature of this source the system described above is not adequate to provide the control required to consistently produce high quality lead salt epitaxial films. This deficiency was not fully recognized until late in the program and steps to remedy the situation did not have a high enough positive impact on the growth capabilities used in this contract work. However, extensive modifications to the system were performed by ITT EOPD funding and the benefits of this work can be appreciated in future contracts. These modifications include temperature control of the auxiliary source and aperture restriction.

Another problem experienced with this growth system was poor vacuum. This problem was partly associated with the excess

overpressure of sulfur described above and also due to the unconfined nature of the evaporation/growth process. Additional problems were due to the large surface area of the substrate heater and incomplete outgassing of same. These problems are also rectified in the modified system which can be used for growth of epitaxial lead salt films on future contracts.

The quality of the lead salt thin films played a decisive role affecting the performance of the thin film ir detectors fabricated in this study. Regardless of process variations, sensitization, or activation procedures, only those films which exibited high Hall mobility ($\gtrsim$5000 $cm^2/V \cdot s$ at 77 K) and moderate p-type carrier concentration ($\approx 10^{17}$ cm^{-3}) were able to yield high performance ir detectors. High quality lead salt epitaxial films proved a necessary but not sufficient condition for the fabrication of high performance ir detectors. Of the many growth runs initiated during the period of this contract, only several produced the necessary high quality lead salt thin films needed to fabricate high performance detectors. The limited control in the growth system described previously was recognized at an early stage as the reason for the poor yield of high quality thin films. However, it was not until the end of the contract that sufficient control of the growth process could be achieved by means of the modifications described.

3.0 DEVICE DEVELOPMENT

The diodes were fabricated using photolithographic and vacuum deposition techniques which permitted the fabrication of devices with geometries not possible with closely spaced metal evaporation masks. Figure 3.0-1 is a photograph of a PbSSe Schottky diode with a 10 mil diameter active area (the centermost dark area). A schematic representation of the device illustrating its structure is shown in Figure 3.0-2. The insulating ring of BaF_2 serves to isolate the electrical leadout from the Schottky barrier to the contact pad in the right-hand corner of the illustration in Figure 3.0-2. The BaF_2 ring also serves as a guard ring preventing surface leakage by passivating the PbSSe surface between the Schottky and ohmic contacts. Also, the possibility of leakage current caused by field crowding at the periphery of the metal contact is eliminated.

3.1 Photolithographic Processing Procedure

The photolithographic processing procedure consists of four steps: (a) delineation of the semiconductor, (b) delineation of the Pt ohmic contact, (c) delineation of the BaF_2 insulating guard ring, and (d) delineation of the Pb Schottky barrier contact. These processing steps are illustrated in Figure 3.1-1.

3.1.1 Semiconductor Delineation

The photolithographic processing in each of the four steps used

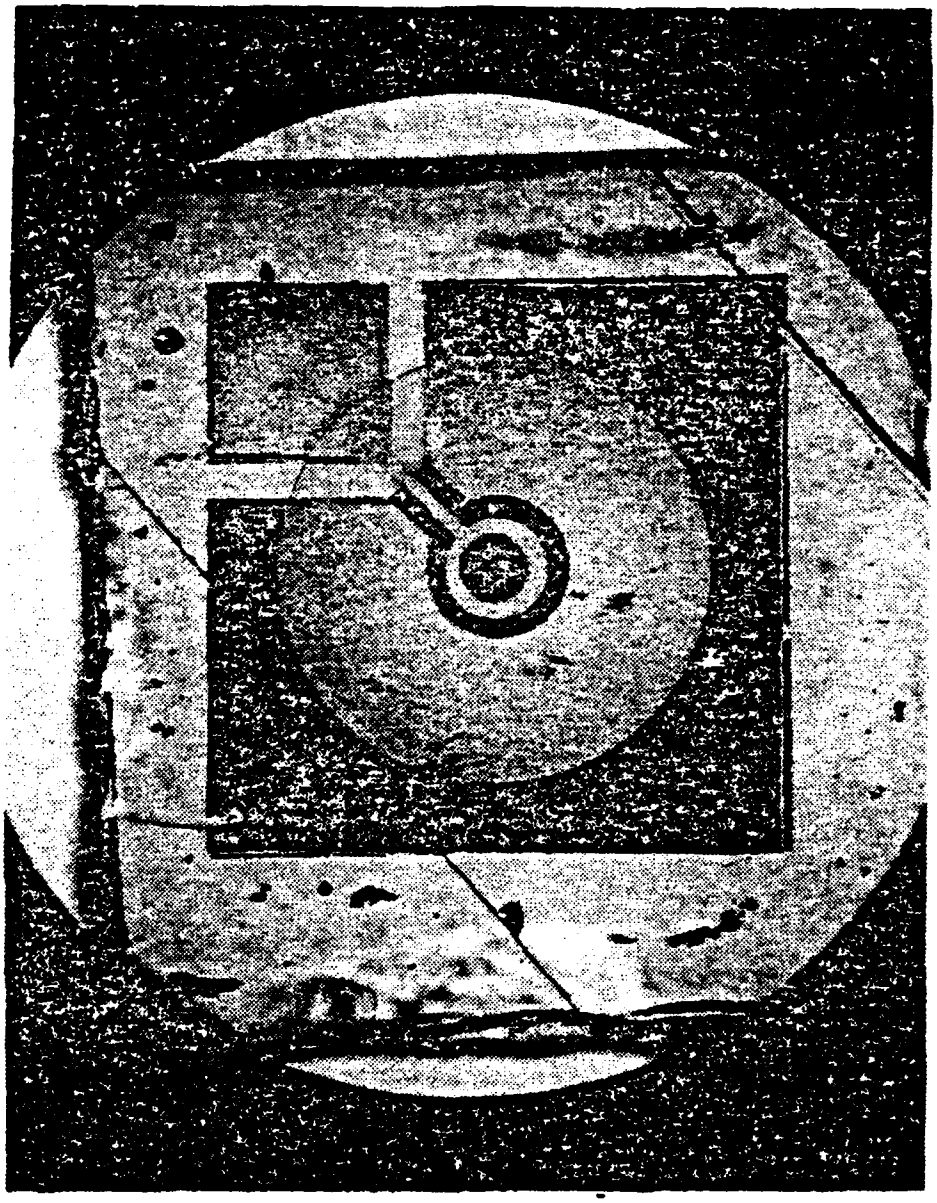

Figure 3.0-1. Photograph of a 10 mil Diameter Pb/PbSSe Schottky Diode.

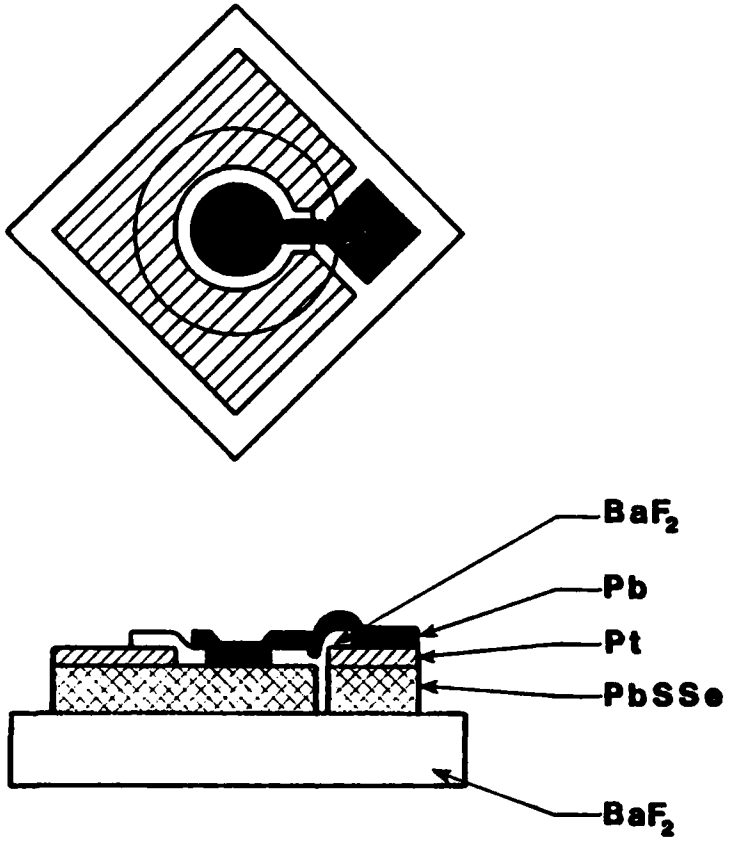

Figure 3.0-2. Top and Cross-Sectional View of the Pb/PbSSe Schottky Diode.

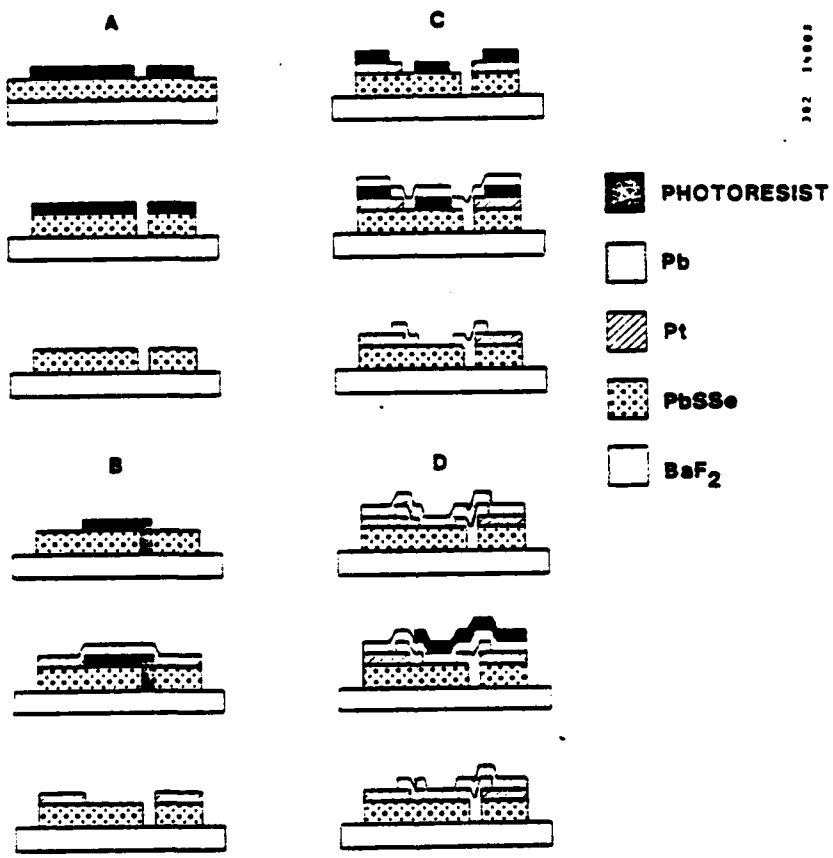

Figure 3.1-1. Pb/PbSSe Schottky Barrier Photodiode Photolithographic Processing Steps Showing the Delineation of (a) Semiconductor, (b) Ohmic Contact, (c) Guard Ring, and (d) Schottky Contact.

Shipley AZ-1350J photoresist. The procedure for applying the resist consisted of spin coating the wafer with one drop at 5000 rpm for 30 s. The coated wafer was then dried in a fresh air circulating oven for 25 min at +90°C. The dried resist was exposed through the appropriate mask using a Kulicke and Soffa 686B mask aligner and ultraviolet (uv) exposure system for 15 s. The exposed photoresist was developed for 30 s in a Shipley MF-312 metal-ion-free developer diluted 1:1 with deionized water. The substrate was then rinsed in deionized water for 15 s to 30 s and blown dry with dry filtered nitrogen gas.

The PbSSe epitaxial film was delineated by applying photoresist and exposing and developing so that the resist covered the desired areas of the film. The resist was then postbaked at +90°C for 25 min. The unprotected epitaxial film was etched using a solution of 7 parts bromine, 10 parts (48%) hydrobromic acid, and 11 parts deionized water by volume. This etch will remove about 5000 Å of PbSSe per second. When the epitaxial layer is etched down to the BaF_2 substrate, it is rinsed in deionized water for 10 s to 15 s. Then the photoresist was removed with acetone and the sample was blown dry with nitrogen gas.

3.1.2 Platinum Delineation

The sample was again coated with photoresist and exposed through a mask which was designed to leave resist where no platinum was

desired. A 1000 Å thick film of platinum was deposited at a rate of 0.5 Å/s by argon ion sputtering a 1 in diameter Pt target using a Millitron I (Commonwealth Scientific Corp) sputter unit. The photoresist and the platinum above it were removed in acetone with ultrasonic agitation.

3.1.3 Barium Fluoride Delineation

The mask for the BaF_2 delineation was configured so that photoresist remained over the active area of the device and also outside the ring which reaches the isolated contact pad. The BaF_2 was deposited to a thickness of about 10,000 Å at 15 Å/s. To prevent a discontinuity in the Pb leadout from the Schottky barrier to the contact pad, the sample was oscillated through an angle of ±20° during the evaporation. After deposition, the resist and the BaF_2 above it were removed with acetone assisted by ultrasonic agitation.

3.1.4 Lead Delineation

The last step of the device processing consisted of evaporating 10,000 Å of Pb over the entire sample. To ensure continuity of the Pb over the edges, the sample was oscillated as for the BaF_2 deposition. Photoresist was applied over the Pb layer and exposed so that the resist remained where it was desired to protect the Pb. A solution of one part acetic acid to one part hydrogen peroxide to five parts deionized water was used to etch only the

unprotected Pb down to the BaF_2 and Pt. The device was then washed 5 min in running deionized water and the photoresist was removed with acetone.

The conditions for evaporation of the Pb are important in determining the final diode characteristics. Diodes which had a relatively rapid Pb evaporation rate (i.e., >10 Å/s) under vacuum conditions of ~10^6 torr produced smooth, metallic-appearing layers. These devices had zero-bias resistance - area product (R_oA) values of 1-5 Ω cm^2 at room temperature, which increased to about 200-300 Ω cm^2 at liquid nitrogen temperature. These diodes exhibit a steep forward bias slope; reverse bias saturation current is 50 μA to 100 μA at 0.4 V at room temperature.

If the Pb is deposited at a very slow rate (i.e., 0.5-1.5 Å/s) with a controlled air or oxygen leak, the Pb layer has a gray, porous appearance. These diodes had R_oA values as high as 1000 Ω cm^2 at room temperature, with less than 10 μA reverse bias saturation current at 0.4 V. However, when placed in a vacuum (or subject to contact pressure), the R_oA of these diodes decreases to 100-200 Ω cm^2. Typical room temperature I versus V characteristics of the two types of diodes are shown in Figure 3.1.4-1. All attempts at passivating or protecting the high R_oA diodes have met with no success. The mechanism responsible for these diodes is not understood and the investigation continued with the more

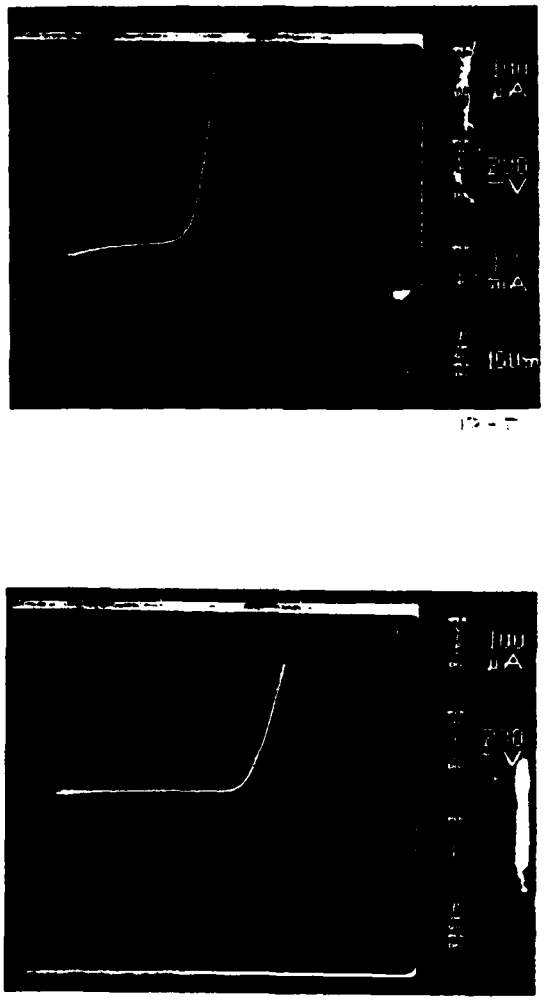

Figure 3.1.4-1. Room Temperature I Versus V Characteristics of Type I and Type II Diodes.

stable diodes produced with a faster Pb evaporation in high vacuum.

4.0 SENSITIZATION

4.1 Chlorine Treatment

The sensitization of the Schottky diodes with chlorine was accomplished prior to the final step of Pb deposition in the device fabrication procedure. The diodes were placed inside a quartz tube furnace along with $PbCl_2$ powder in an open vessel and heated to +300°C for 0.5 h to 1.0 h. Dry nitrogen was passed through the tube to aid in the transport of the $PbCl_2$ vapor downstream over the exposed PbSSe surface of the partially completed diodes.

Figure 4.1-1 shows the Auger surface analysis scan of the PbSSe film before and after the $PbCl_2$ treatment. The chlorine was located mainly in a layer 20 Å thick, beyond which the Cl concentration decreased rapidly but extended at low concentration to a depth of 100 Å (see Figure 4.1-2). The increase of the chlorine at the surface coincides qualitatively with a decrease in the sulfur content. There was also an increase in oxygen content at the surface as a result of the $PbCl_2$ treatment. Carbon residue from the photoresist and developer processing was found on the surface of the PbSSe. In order to remove this residue, some samples were plasma etched, but the finished diodes were not improved. The majority of high performance diodes were fabricated with Pb deposited on the carbon contaminated surface. However, it was determined that those diodes which were chlorine treated had

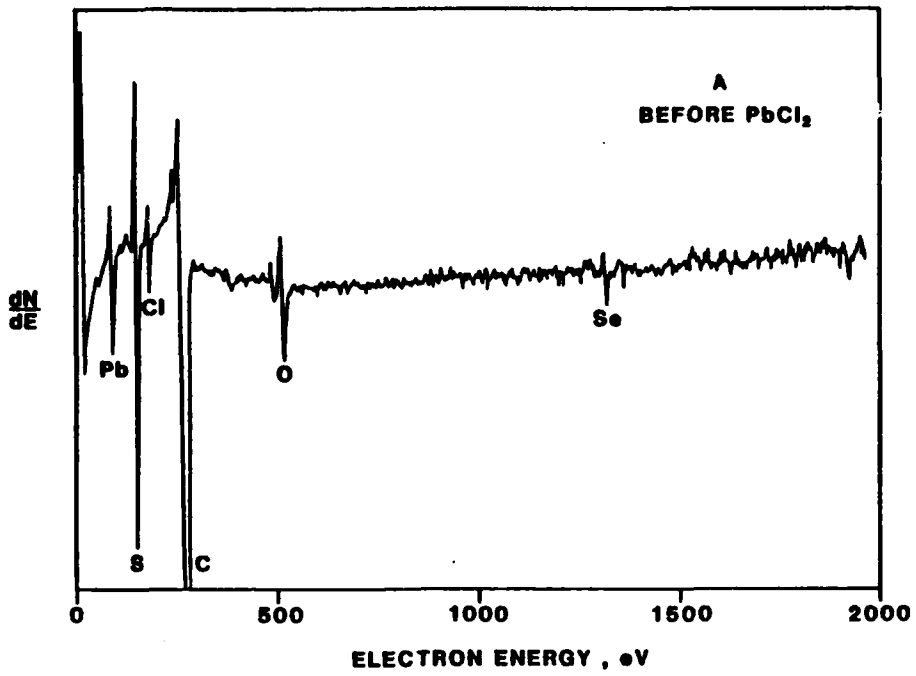

a. Prior to $PbCl_2$ treatment. Slight chlorine peak is a result of air exposure. Large carbon peak is indicative of residue from photoresist and developer.

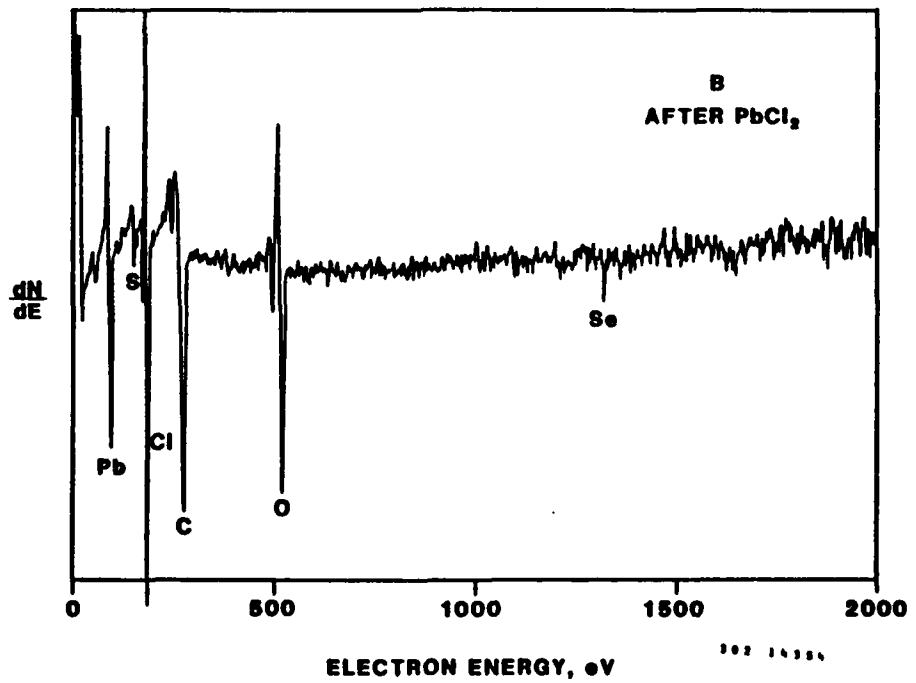

b. After $PbCl_2$ treatment. Note in particular increase of chlorine and decrease in sulfur as compared to (a).

Figure 4.1-1. Auger Spectrum of PbSSe Surface.

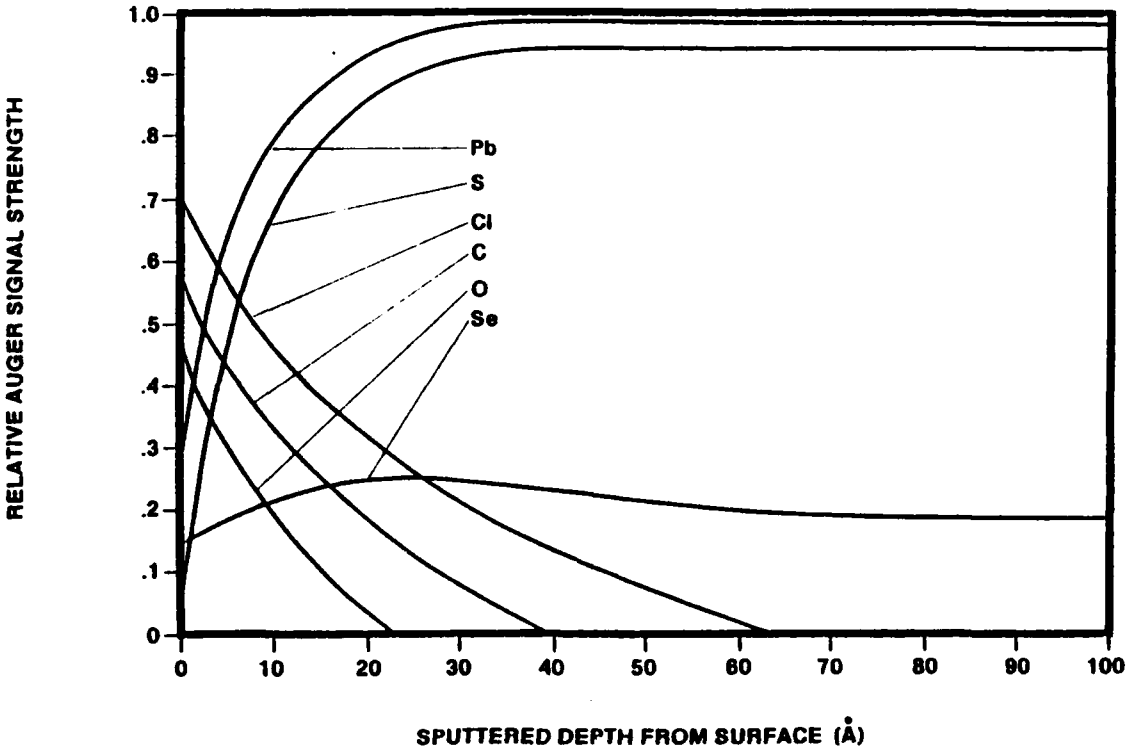

Figure 4.1-2. Depth Profile of Chloride Treated PbSSe Surface.

less carbon than diodes which were untreated. More work will be required to assess the effect of the carbon residue on detector performance.

Although Cl was effectively introduced into the PbSSe epitaxial layer by soaking in a liquid chlorine bleach and thoroughly rinsing in DI water (see Figure 4.1-3), this did not yield results as good as those with $PbCl_2$. Also, introducing Cl into the vacuum system during the Pb evaporation proved ineffective. This method, however, has not been tested to its fullest and is deserving of a more complete investigation.

Diodes fabricated from material chlorinated with $PbCl_2$ showed improved R_oA values and yields, as compared to diodes which did not receive the $PbCl_2$ treatment. As an example of this result, Figure 4.1-4 shows the I versus V characteristics of two 10 mil diameter active area diodes at room temperature. Both diodes were fabricated from the same growth; diode 12-D received the chlorination treatment while diode 12-5 did not.

The yield of 10 mil diameter active area diodes was good using the chlorination process; however, the yield of 80 mil diameter active area diodes was uncertain, probably due to epitaxial layer defects. Improved 80 mil diode yield was achieved using an anneal process.

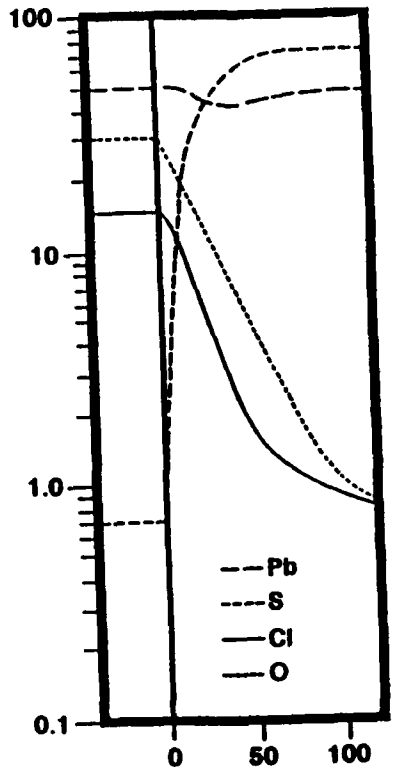

a.

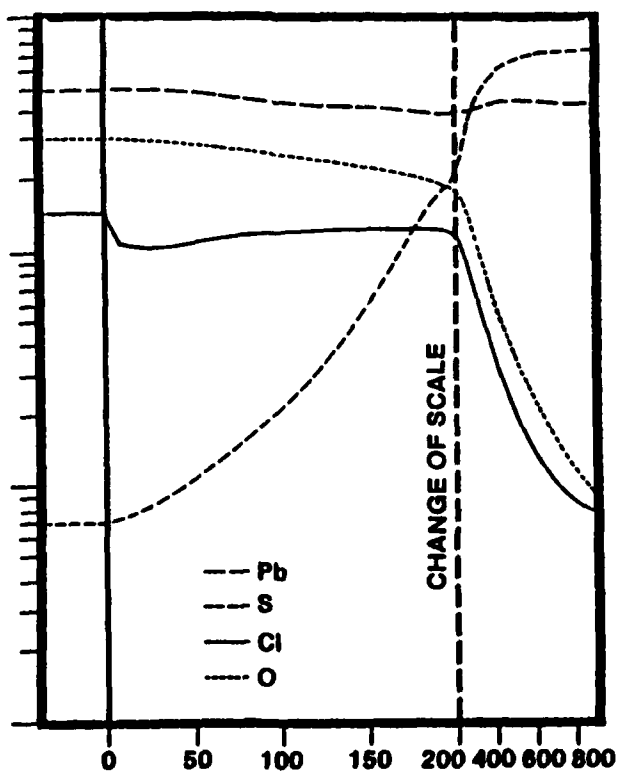

b.

Figure 4.1-3. Sputter Profile of PbSSe Liquid Chlorine Bleach Treated for (a) 1 h and (b) 17 h.

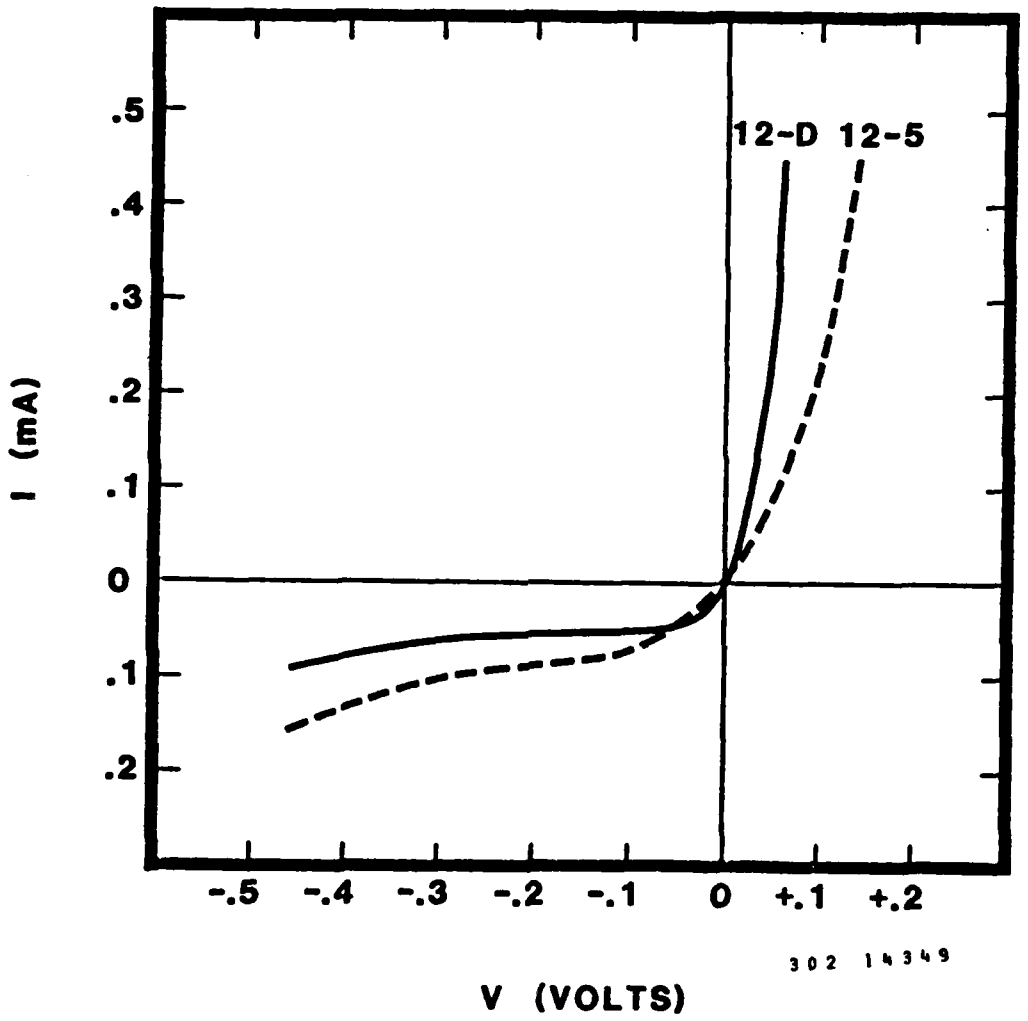

Figure 4.1-4. Dark I versus V characteristics at 300 K of Pb/PbSSe diodes with active area 5 x 10^{-4} cm^2. Both diodes were fabricated from the same growth but diode 12-D was treated at +300°C for 0.5 h in the presence of $PbCl_2$ vapor before the Pb contact evaporation; diode 12-5 was untreated.

4.2 Heat Treatment

The yield of 80 mil diameter diodes was significantly improved by heating the processed diodes at +260°C (which is below the lead melting point of +328°C) for 30 min in an air convection oven. Figure 4.2-1 shows the effectiveness of the technique. This method works well regardless of prior treatments (i.e., chlorination or plasma etching); hence, the annealing treatment has the desirable characteristic of being very forgiving to process variations which may occur during device fabrication.

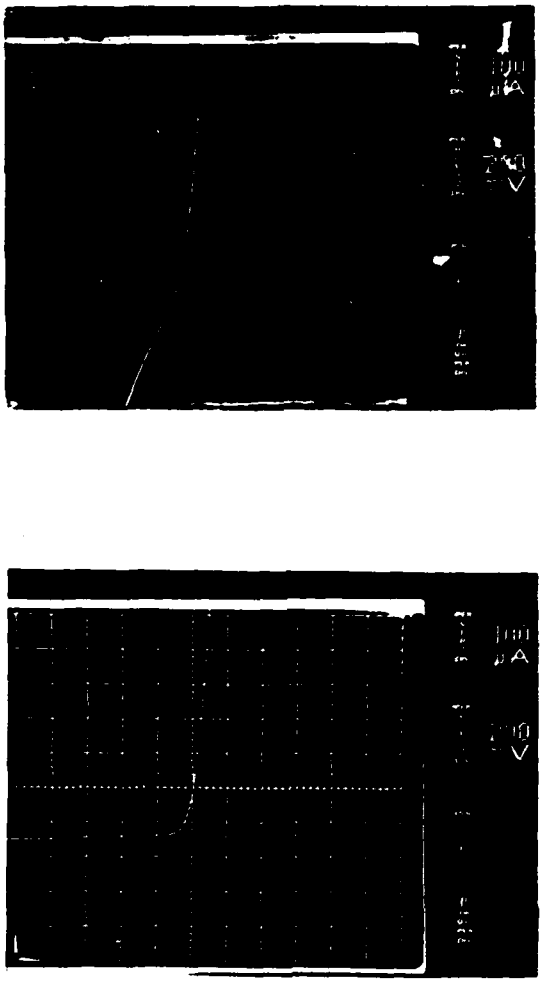

Figure 4.2-1. Diode I Versus V Characteristics Before and After Heat Treatment at +260°C for 1/2 h.

5.0 MEASUREMENTS

5.1 Material Characteristics

5.1.1 Spectral Transmission

All grown epitaxial layer material was characterized using transmission data obtained with a Perkin-Elmer model 599 spectrophotometer (see Figure 5.1.1-1). The results were used to determine the expected spectral response of the finished device, the composition of the material (i.e., S/Se ratio), and the film thickness.

An estimate of the room temperature energy band gap is determined to be equivalent to the corresponding photon energy at the shortest wavelength where the epitaxial film has one-half its local maximum transparency. From this result it is possible to infer the S/Se atomic percent ratio. By measuring the interference fringes the film thickness is determined by

$$t = m\lambda/2n_i \qquad (5\text{-}1)$$

where m is the interference order, n_i is the refractive index, and λ is the radiation wavelength. Typical thicknesses of the films were 2 μm to 3 μm.

5.1.2 Van der Pauw

A sample from each growth was characterized using the Van der Pauw

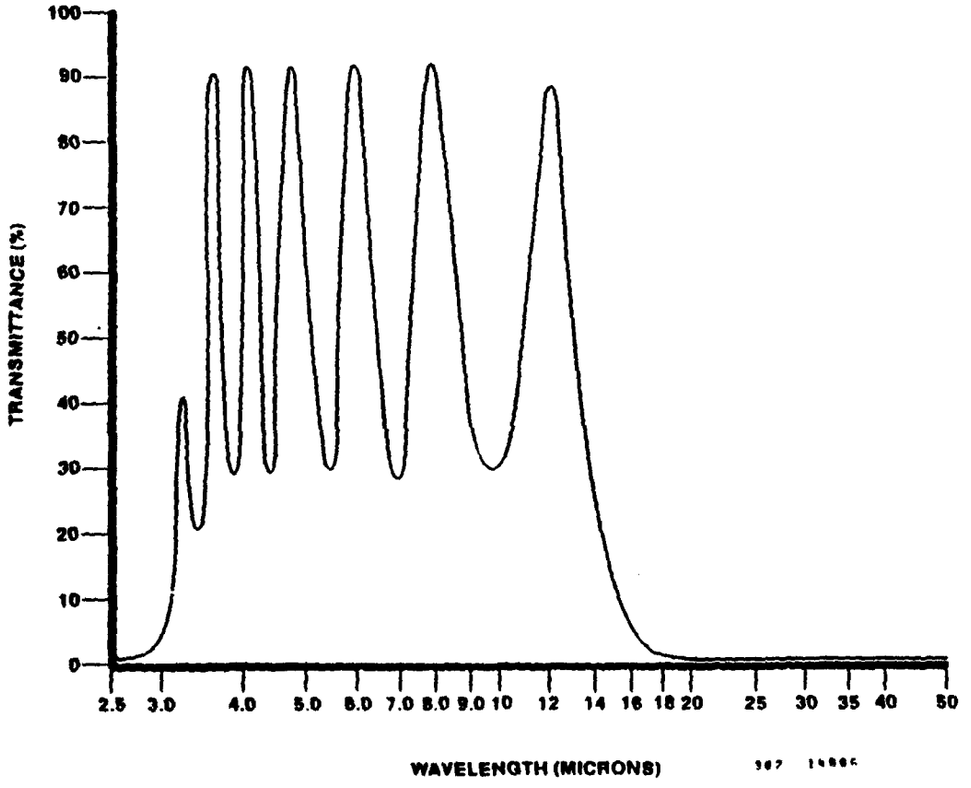

Figure 5.1.1-1. Spectral Transmission Characteristic of a Typical PbSSe Epitaxial Layer on BaF_2 Substrate.

method to measure the Hall coefficient and resistivity. From this data, Hall mobility, carrier type, and carrier concentration were determined. Four Pt ohmic contact pads were deposited on the PbSSe epitaxial layer. Electrical contact to the ohmic pads was made using indium covered probes. Measurements were taken both at room temperature and at liquid nitrogen temperature. PbSSe epitaxial material with p-type carrier concentrations of $1\text{-}3 \times 10^{17}$ cm^{-3} with a mobility of 10,000 $cm^2\ V^{-1}\ s^{-1}$ at 80 K has been obtained. Lead salt films having these characteristics produced the best detectors. Films having carrier concentrations greater than 10^{18} cm^{-3} and Hall mobilities of only a few thousand $cm^2 \cdot V^{-1} \cdot s^{-1}$ at 80 K invariably produced inferior detectors regardless of the post growth processing procedures.

5.2 Device Characteristics

5.2.1 Resistance - Area Product

Zero-bias resistance (R_O) which is the slope of the I versus V characteristic at zero bias was measured using a Tektronix 576 curve tracer. Zero-bias resistance - area products (R_OA) for 80 mil diameter active area diodes varied between 0.2 and 1.0 $\Omega\ cm^2$ at room temperature. At 77 K, R_OA values as high as 2000 have been measured although typical values for annealed 80 mil diodes were 200-1000 $\Omega\ cm^2$ (see Figure 5.2.1-1).

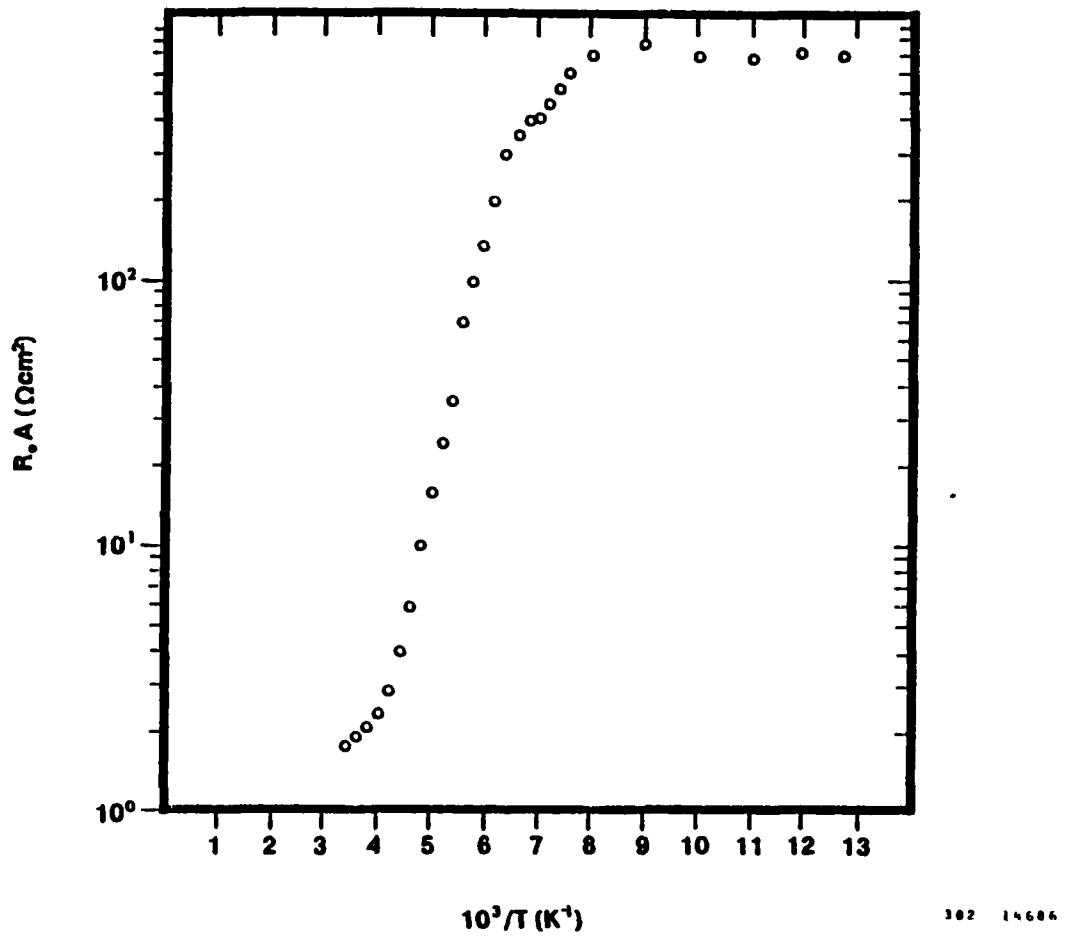

Figure 5.2.1-1. Temperature Dependence of the Zero-Bias Resistance - Area Product for an 80 mil Diameter Pb/PbSSe Schottky Barrier Diode.

5.2.2 Current-Voltage Characteristics

The variation with temperature of the forward current voltage characteristics of an 80 mil diameter Pb/PbSSe Schottky diode is shown in Figure 5.2.2-1.

The forward current (at constant forward bias) has been observed to decrease with increasing temperature from 77 K to 100 K before the forward current begins to increase again with increasing temperature from 100 K to 300 K (see Figure 5.2.2-2). This effect cannot be presently explained and will be investigated in the future.

5.2.3 Spectral Response

Spectral response measurements of processed PbSSe photodiodes have been made using a Perkin-Elmer 12C ir spectrophotometer. Figure 5.2.3-1 shows a typical relative spectral response of a Pb/PbSSe Schottky barrier junction photodiode cooled to 80 K. A cut-off wavelength at 4.7 μm indicates that the PbSSe material in this device is sulfur rich. The use of sulfur alone during growth of epilayer material from a $PbS_{0.5}Se_{0.5}$ source produced films of $PbS_{1-x}Se_x$ with x as small as 0.2. To achieve the desired long wavelength cutoff, the auxiliary source producing chalcogenide overpressure during film growth must be carefully controlled (see Section 2.0).

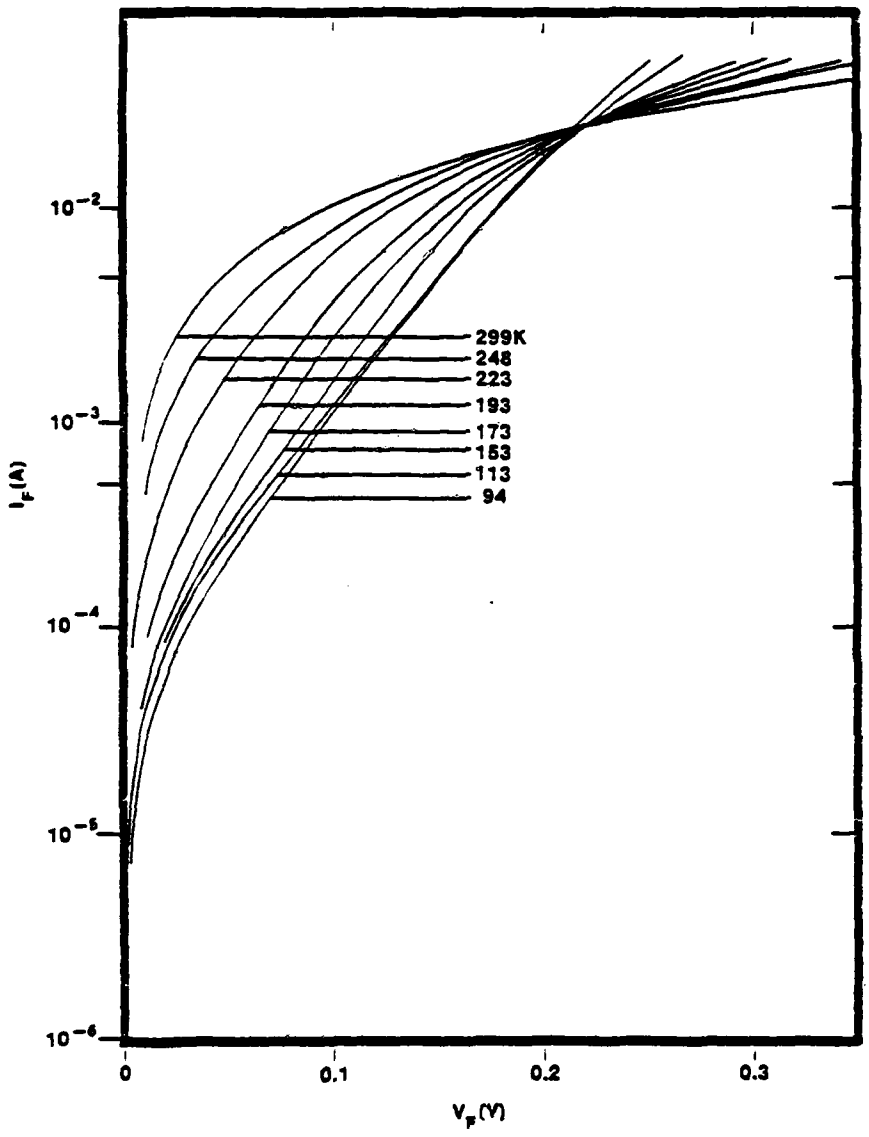

332 14682

Figure 5.2.2-1. Forward I Versus V Characteristics as a Function of Temperature for a Pb/PbSSe Schottky Diode.

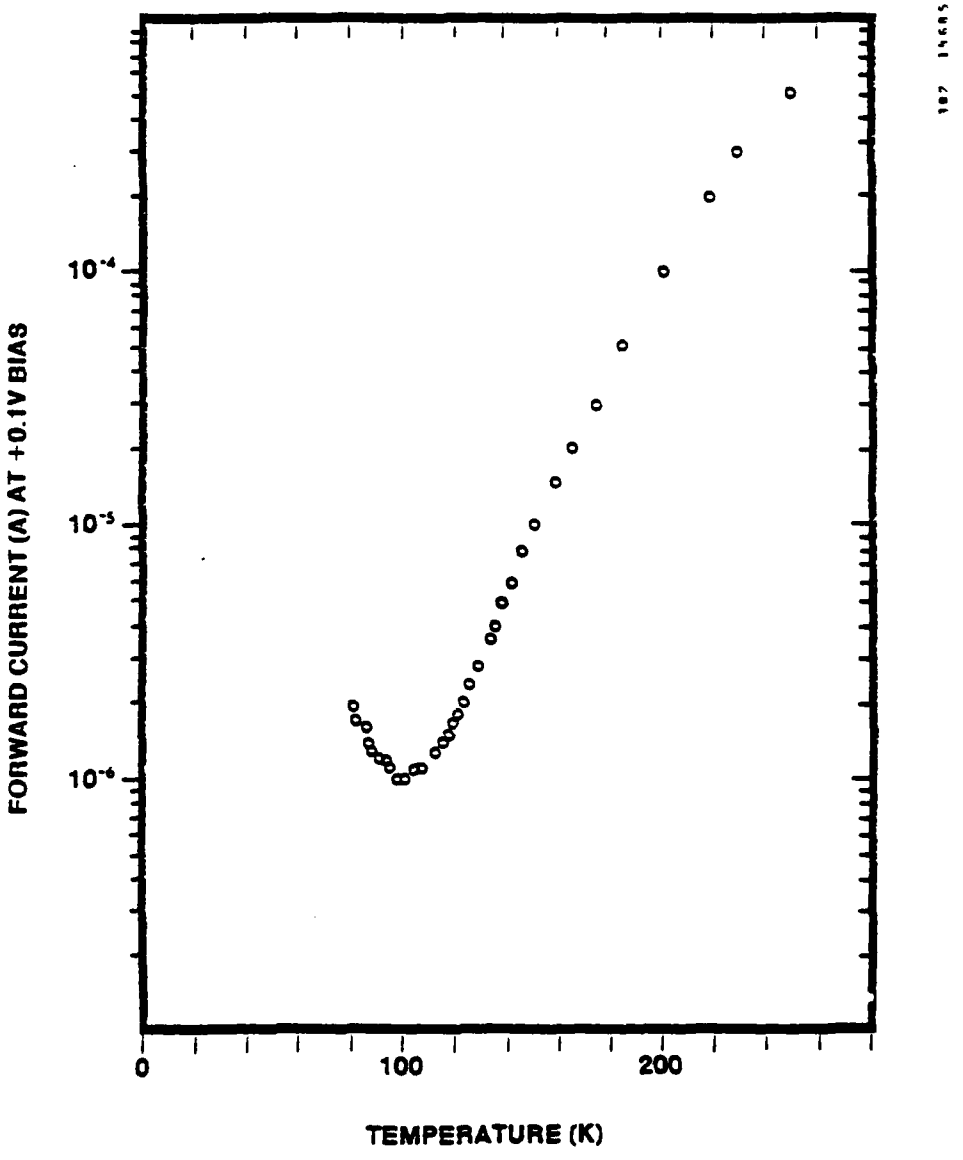

Figure 5.2.2-2. Temperature Dependence of the Forward Current at a Bias of +0.1 V for a Pb/PbSSe Schottky Barrier Diode.

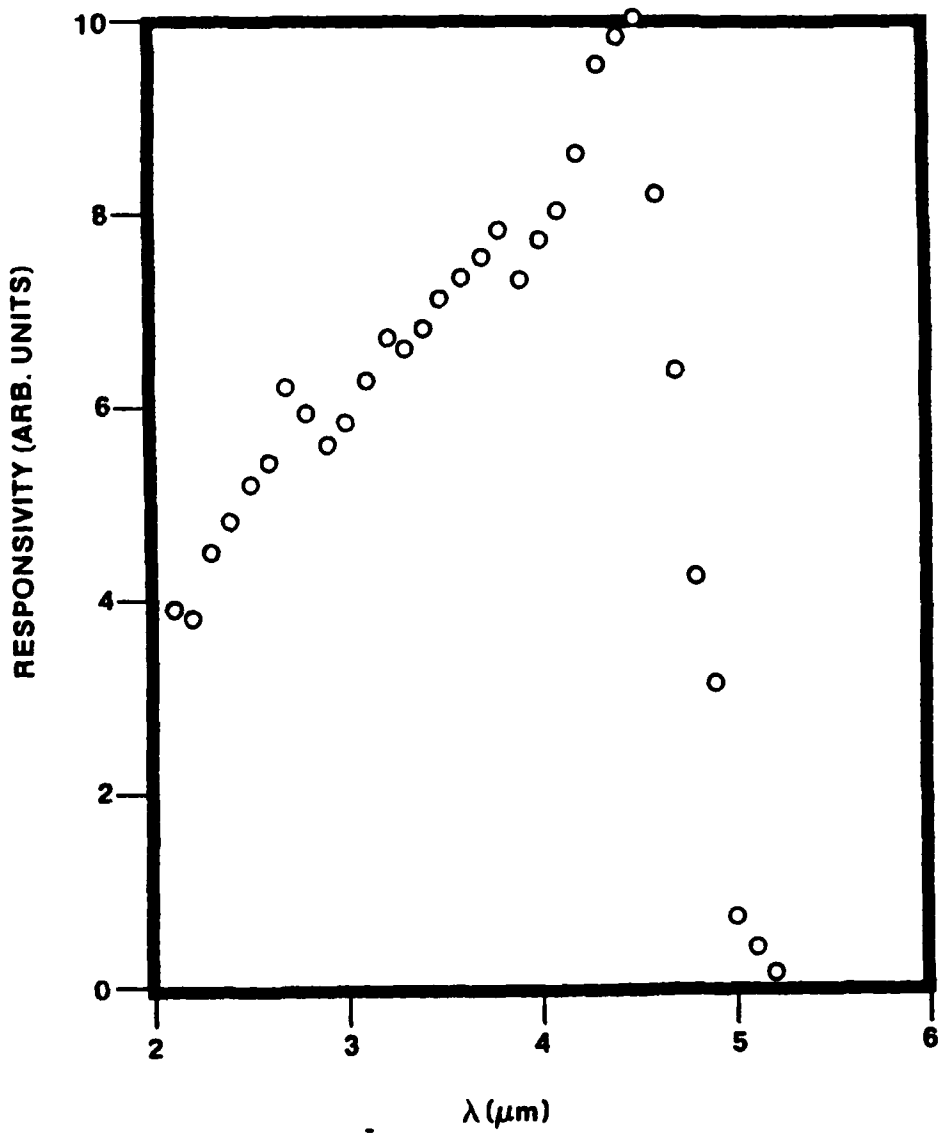

Figure 5.2.3-1. Spectral Response of a Pb/PbSSe Schottky Barrier Photodiode at 77 K.

5.2.4 Quantum Efficiency

One of the important parameters characterizing the performance of an ir detector is the quantum efficiency. This is simply a measure of the ratio of the number of electrons collected by the detector to the number of photons incident on the detector. Ideally, a monochromatic radiation source is used to provide the incident photons. In this case the photon flux (number of photons per unit time) incident upon the detector is obtained by a radiometric power measurement using a Laser Precision Corp. model RS-3960 radiometer. The incident power at the detector is measured and converted to photon flux at the detector using the energy per photon relation: $E = hc/\lambda$. The output current of the detector is measured and quantum efficiency is calculated by taking the ratio of output current to input photon flux.

However, problems were experienced in achieving a suitably intense monochromatic radiation input to the detector with the available equipment. An alternate and more widely used procedure was adopted to obtain an average value for the quantum efficiency over the entire spectral response of the detector. A 500 K blackbody radiation source was used to provide the incident radiation at the detector. The spectral output of the blackbody source was convolved with the spectral response of an ir detector. Thus, measurements of input radiant power and output current were used to calculate the average quantum efficiency of the detector. A simple low resolution numerical integration procedure was used in the

convolution process. Results obtained with this technique gave values of 60-70% for the quantum efficiency of the best detectors tested. These detectors also exhibited high performance in terms of detectivity (see paragraph 5.2.5).

5.2.5 Detectivity

The detectivity was also measured using the blackbody source described in the previous subsection. The detector was mounted in an evacuated dewar at 77 K and illuminated through an Irtran 2 window and BaF_2 detector substrate. A digital voltmeter was used to measure the root-mean-square (rms) photovoltage output response (V_S) to 700 Hz incident 500 K blackbody radiant power and the detector noise voltage (V_N) was determined with a Hewlett-Packard model 302A wave analyzer in a 7 Hz bandwidth (Δf). The rms signal voltage was also measured with a wave analyzer in many cases to check the validity of using the digital voltmeter for this purpose. In all cases tested, the wave analyzer and voltmeter agreed to within a few percent. The 500 K blackbody detectivity (D^*_{bb}) was calculated using the formula:

$$D^*_{bb} = \frac{\sqrt{\Delta f}}{H\sqrt{A_D}} \cdot \frac{V_S}{V_N} \qquad (5\text{-}2)$$

where H is the rms value of the irradiance falling on the detector of area A_D. For high quality diodes D^*_{bb} was in the range of 10^9 to 10^{10} cm $Hz^{1/2}$ W^{-1} at 77 K. The vast majority of detectors fabricated had $D^*_{bb} < 109$ cm $Hz^{1/2}$ W^{-1} at 77 K. The very best detectors (always from high mobility epitaxial films) had $D^*_{bb} \approx 2 \times 1010$ cm $Hz^{1/2}$ W^{-1} which yields $D^*_{\lambda_p} \gtrsim 10^{11}$ cm $Hz^{1/2}W^{-1}$ at 77 K, where λ_p = the wavelength at which maximum responsivity occurs.

6.0 DISCUSSION

The presence of chlorine at the Pb/PbSSe interface improves the yield of high performance devices. Also, it was determined in this work that the best treated diodes had higher R_oA values than the best untreated diodes. By considering the different models of the Pb/PbSSe photodiode (e.g., pn junction, Schottky, and metal-insulator-semiconductor (MIS)), there are several possible mechanisms by which the chlorine could be responsible for improved diode properties.

If the grown PbSSe epitaxial layer contained any surface Pb precipitates and/or other defects and impurities, the Pb Schottky contact would be shorted by these leakage paths across the metal-semiconductor junction and thus degrade R_oA. Indeed, evidence for this has been obtained in this work. Pb Schottky contacts (10 mil diameter) were deposited at random over the surface of a PbSSe film which exhibited sections of haziness and visible point defects. An ohmic Pt contact was deposited at one end of the film. Pb contacts which were either covering hazy sections of the film or point defects exhibited R_oA values which were smaller by more than a factor of 10 than those for contacts in regions where no defects were visible. When such material is exposed to chlorine, the Pb precipitates at the surface could react with the chlorine to form insulating $PbCl_2$ at these defects and thus improve the diode. More likely, however, the entire surface has

been affected by the chloride treatment process and it is not unreasonable to expect $PbCl_2$ and other compounds to be present in greater or lesser amounts. In addition, as these diodes have been processed using several steps involving photoresist, carbon and oxygen have been detected on the surface of the PbSSe before the Pb contact was deposited.

Depth profiling has shown the contaminants intermixed with the first few monolayers of the PbSSe epitaxial layer. For most samples tested, the concentration of the carbon and oxygen was down to 50% of surface maximum at a depth of 10 Å and 90% of maximum at a depth of 20 Å from the surface. This surface layer could prevent a true Schottky barrier from being formed at the metal-semiconductor interface if the contaminants remained isolated at the interface after contacting with lead. Auger depth profile data has been inconclusive in determining the details of the composition at the interface because of profile broadening due to sputtering effects.

It is also possible that the chloride treatment produces a pn junction. The chlorine could act as a donor if it were substituted for either sulfur or selenium in the PbSSe lattice thus changing the material from p-type to n-type. This would lead to a pn junction near the surface of the epitaxial PbSSe layer and the Pb layer would act as an ohmic contact to the n-type PbSSe.

However, this pn junction model does not appear to be valid for these diodes. The barrier heights of the junction have been measured using the $1/C^2$ versus V method on completed diodes which have seen different chloride treatments. Within experimental error, there is no change in barrier height between diodes which have seen no chloride treatment and those which have been chloride treated at temperatures up to +250°C for 1/2 h (see Figure 6.0-1). Therefore, it is concluded that the standard pn junction model is not valid for these PbSSe diodes.

It is proposed that the model which best fits the observed behavior of the Pb/PbSSe system is the MIS model wherein the insulator is very thin (~10 to 20 Å).[8] Furthermore, the space-charge layer of the p-type PbSSe semiconductor (under the insulator) is inverted. Consequently, a pseudo pn junction is thus formed.

The thickness of the interfacial layer is important in determining the behavior of the MIS system. If it is very thin, tunneling takes place easily through it. This will be so if the thickness is of the order of 10-20 Å; thicker insulating layers will behave as series-resistance elements.

When the semiconductor surface layer is inverted, the device is a minority-carrier tunneling MIS system because the principal tunnel

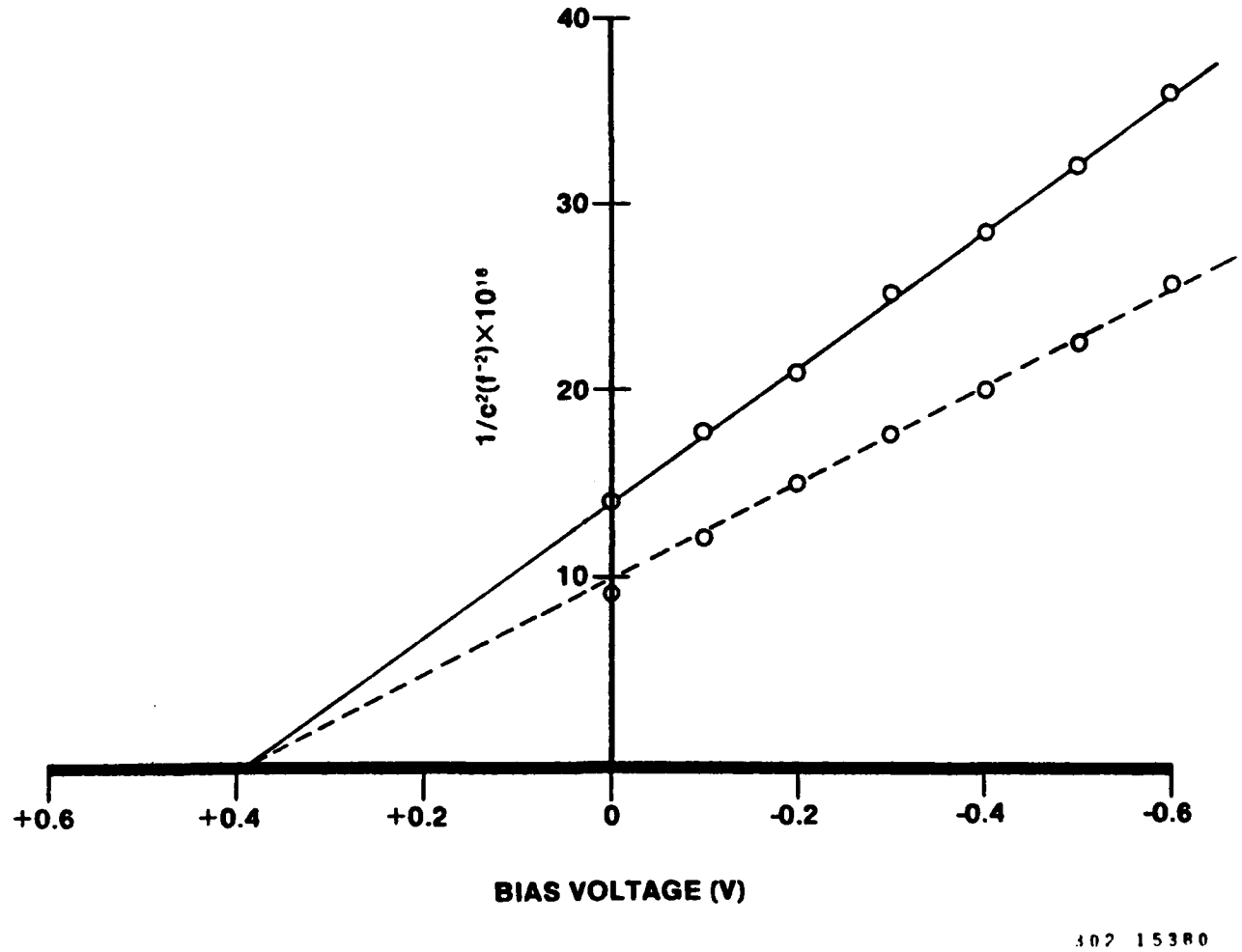

Figure 6.0-1. $1/C^2$ Versus V Plot for Pb/PbSSe Schottky Diodes at 77 K Having Barrier Heights of 0.39 eV. The Solid Line Is for Untreated PbSSe and the Broken Line Is for PbSSe Heated at +200°C for 0.5 h in the Presence of $PbCl_2$ Before the Evaporation of the Pb Schottky Contact.

current is between the metal and the conduction band (which is the minority carrier band in the p-type semiconductor).

For a given thickness of the insulating layer, at low forward bias the carrier concentration at the semiconductor surface is fixed as though doped by a diffusion process and the MIS diode operates as a pseudo pn junction. At high forward bias, the current flow is limited by the ability of the electrons to tunnel, and the effect of the latter is to act as a series resistance in the circuit.

The current-voltage characteristics at a given temperature are indistinguishable whether the model is that of a Schottky barrier or a pn junction. Both yield an expression of the type

$$J = J_o(eqV/nkT - 1) \qquad (6\text{-}1)$$

where J_o is the reverse saturation current density.

If the dominant mechanism is due to tunneling, the current will be given by

$$J = A \cdot e^{\beta V} \qquad (6\text{-}2)$$

All models yield currents which depend exponentially on the applied voltage.

The models become distinguishable when the temperature dependence of the I-V characteristics is considered.

In the case of a Schottky barrier (thermionic emission mechanism), the coefficient is

$$J_o = AT^2 e^{-\phi_b/kT} \tag{6-3}$$

wherein A is the modified Richardson constant and ϕ_b is the barrier height.

Note that the band gap of the semiconductor does not enter into the equation. It appears indirectly through ϕ_b.

In the case of a pn junction, wherein the Shockley diffusion model holds, the reverse saturation current is:

$$J_o = qn_i^2\left(\frac{D_p}{N_D L_p} + \frac{D_n}{N_A L_n}\right) \tag{6-4}$$

where

N_D = donor impurity density

N_A = acceptor impurity density

D and L = diffusion coefficient and diffusion length, respectively, where the subscripts p and n refer to holes and electrons

In the case of a pn junction wherein thermal generation-recombination in the space-change region plays a dominant role, then the reverse saturation current is:

$$J_o = \frac{qW}{\tau_d} n_i \tag{6-5}$$

where

W = depletion-layer width

τ_d = lifetime

if there is generation-recombination in the space-charge region.

In either case, the band gap of the semiconductor enters through the intrinsic carrier concentration:

$$n_i = CT^{3/2} e^{-E_g/2kT} \qquad (6\text{-}6)$$

The relationship between J_o and R_oA is given by

$$R_oA = \left(\frac{\partial J}{\partial V}\bigg|_{V=o} \right)^{-1} = \frac{nkT}{qJ_o} \qquad (6\text{-}7)$$

where J is taken from equation 6-1.

A plot of ln (R_oA) versus 1/T (Figure 5.2.1-1) shows three distinct regions having slopes of ≈Eg/k, Eg/2k, and O respectively. This data was taken from a typical high performance detector fabricated during this program.

This result is consistent with the pn junction model with J_o given by equations 6-4 and 6-5; the diffusion limited behavior (equation 6-4) is dominant at high temperature (1/T small), and the depletion limited behavior (equation 6-5) is dominant at lower temperature

(1/T large). For 1/T very large the slope is zero and shunt resistance effects dominate; R_oA stays constant with further decreases in temperature. This behavior can also be interpreted as evidence of the tunnelling mechanism dominating in the low temperature range (see equations 6-7 and 6-2).

We see that the behavior of R_oA versus temperature, for detectors fabricated in this program, most closely approximates that expected for the p-n junction model, not the Schottky barrier model; and that shunt resistance or tunnelling effects dominate in the low temperature regime (i.e., $T \leq 100K$). Furthermore, the chlorination process does not alter the barrier height, but instead provides a thin barrier to majority carriers (reduces leakage) which minority carriers can tunnel through. The tunnelling efficiency for the minority carriers is high enough so that the I versus V characteristics of the device are characterized by a pn junction model except at low temperature.

Note however, none of the models or equations discussed above predict a minimum for the current versus temperature at constant bias voltage as is shown in Figure 5.2.2-2. The result is atypical, but it is a real effect in some of the devices fabricated in this program. The anomalous nature of this result is cause for concern and is clear evidence of our lack of complete understanding of the mechanisms governing the behavior of these devices.

A different method developed for sensitizing Pb/PbSSe Schottky diodes is by annealing completed diodes. Using this method, high yields of high quality devices have been obtained. This process has been investigated in the past, primarily by H. Holloway at Ford Research, using 100°C-150°C for PbSnSe Schottky diodes.[9] This low temperature anneal was found to be ineffective for improving Pb/PbSSe diodes, however, a high temperature anneal (200°C-300°C) is very effective when used on Pb/PbSSe diodes. The explanation for the effectiveness of this process for PbTe diodes was originally explained by Holloway as a dissolution of the detrimental interfacial oxide into the Pb contact. ITT EOPD's Auger depth profile analysis results show a different mechanism responsible for the improvement in the performance of Pb/PbSSe diodes. The Pb/PbSSe interface of heat treated diodes is considerably broadened compared to untreated diodes. There are three distinct regions: lead contact region, lead salt region with high lead content, and the grown epitaxial layer lead salt material (see Figure 6.0-2). These results can be interpreted as leading to a structure consisting of an ohmic lead contact, n-type lead salt material, and p-type lead salt epitaxial layer. Hence, these diodes are no longer Schottky diodes having an inverted space charge region giving rise to a psuedo pn junction, but instead, the heat treatment has produced a diffusion process resulting in a pn^+ junction device.

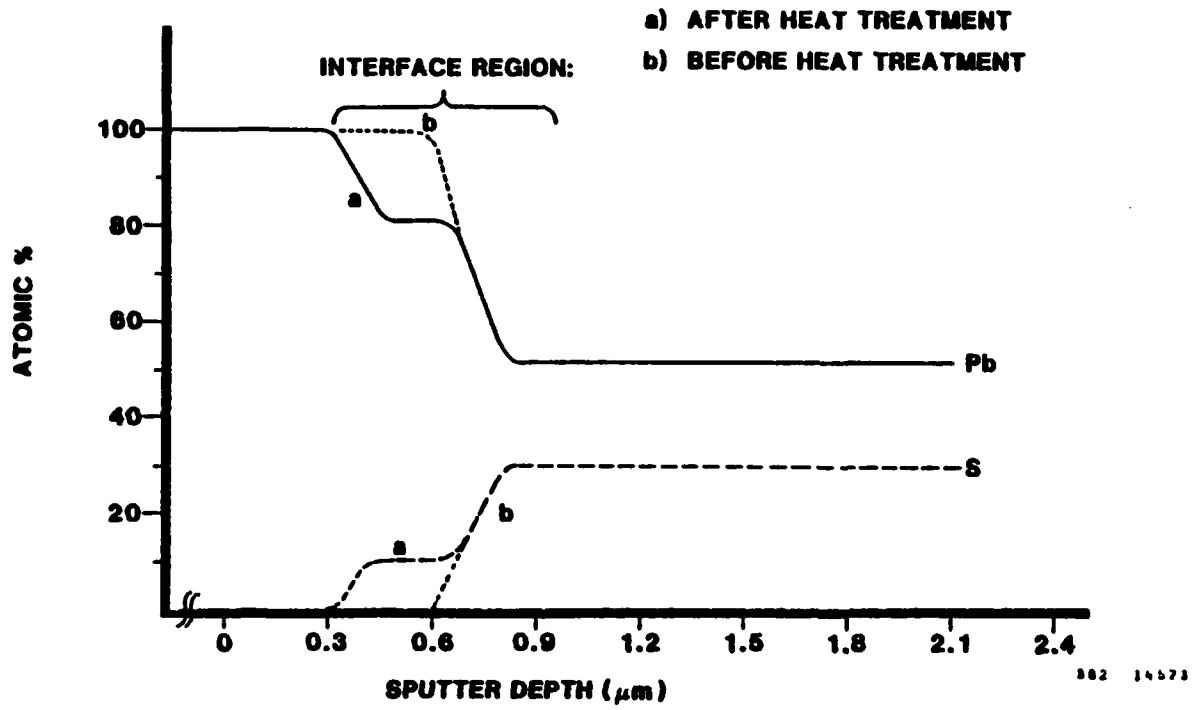

Figure 6.0-2. Auger Depth Profile Through Pb/PbSSe Interface.

13907

7.0 CONCLUSIONS

The establishment of the technology at ITT EOPD for the growth, fabrication, and evaluation of Pb/PbSSe Schottky photodiodes has been initiated. Although devices with BNL values of $D_\lambda^* = 1 \times 10^{11}$ cm $Hz^{1/2}$ W^{-1} have already been achieved, consistent yields remain a problem. High quality epitaxial layer material is of paramount importance in achieving good devices. The problems at the present time lie in the nonuniformity and control of stoichiometry and doping of the PbSSe epitaxial layer material. The development of methods of improving or sensitizing the devices has helped increase yields. The first method uses a chloride treatment process which forms an MIS type device. Also, during the work on this program a new method was developed which gave significant improvement over the chloride treatment method. This method involved annealing the finished devices, and evidence points to a diffused pn junction as the mechanism.

Several possibilities exist for future investigation. The mechanism of the slow Pb deposited type II diodes requires more study. Instead of using chlorine in the sensitization of the Pb/PbSSe interface, other halides such as fluorine, bromine, and iodine may have other effects. Also, introducing Cl before or during the Pb evaporation may improve the chlorination process. Calcium fluoride insulating guard rings instead of barium fluoride may improve the quality of the device as it has better mechanical properties

and is much less water soluble than BaF_2. The heat treatment process can be modified by heating the samples during Pb deposition. This method woud eliminate the effect of oxygen and other impurities introduced during heat treatment in air.

8.0 REFERENCES

1. Schoolar, R. B., J. D. Jensen, and G. M. Black. "Composition-Tuned PbS_xSe_{1-x} Schottky-Barrier Infrared Detectors," Applied Physics Letters, (31) (1977), pp 620-622.

2. Holloway, H. "Thin-Film IV-VI Semiconductor Photodiodes," Physics of Thin Films, ed by G. Hass and R. E. Thun, (11), Academic Press, Inc., New York (1980), pp 105-203.

3. Holloway, H., and E. M. Logothetis. "Epitaxial Growth of Lead Tin Telluride," Journal of Applied Physics, (41) (1970), pp 3543-3545.

4. Lopez-Otero, A. "Hot-Wall Epitaxy," Thin Solid Films, (49) (1979).

5. Bleicher, M., H. D. Wurzinger, H. Maier, and H. Preier. "n-Type PbS and $PbS_{1-x}Se$ Layers Prepared by the Hot-Wall Epitaxy," Journal of Material Science, (12) (1977), pp 317-322.

6. Hohnke, D. K., H. Holloway, M. D. Hurley, S. W. Kaiser, P. V. S. Rao, A. J. Varga, A. E. Asch, and D. A. Gorski. "Development of PbTe and (Pb,Sn)Te Photovoltaic Detectors by Vacuum Sublimation," U.S. Army Night Vision Laboratory Final Report, contract DAAK02-72-C-0391 (1973).

7. Hohnke, D. K., H. Holloway, M. D. Hurley, S. W. Kaiser, P. V. S. Rao, A. J. Varga, A. E. Asch, and D. A. Gorski. "Lead Telluride Photodiodes for Operation at 170 K," U.S. Army Electronics Night Vision Laboratory Final Report, contract DAAK02-73-C-0225.

8. Schewchun, J., D. Burk, and M. B. Spitzer. "MIS and SIS Solar Cells," IEEE Transactions on Electron Devices, (ED-27) (1980), pp 705-716.

9. Asch, A. E., D. A. Gorski, D. K. Hohnke, H. Holloway, M. Hurley, and K. F. Yeung. "Lead Tin Telluride and Lead Tin Selenide Thin Film Detectors," U.S. Army Night Vision Laboratory Final Report, contract DAAK02-74-C-0124.

DISTRIBUTION LIST

Dr. A. C. Bouley
Naval Surface Weapons Center
Code R45
White Oak, Silver Spring, MD 20910

Dr. T. K. Chu
Naval Surface Weapons Center
Code R45
White Oak, Silver Spring, MD 20910

Dr. Howard Lessoff
Naval Research Laboratory
Code 6820
Washington, DC 20375

Mr. H. S. Riedl
Naval Surface Weapsons Center
Code R45
White Oak, Silver Spring, MD 20910

Code R45 (10 copies)
Naval Surface Weapons Center
White Oak, Silver Spring, MD 20910

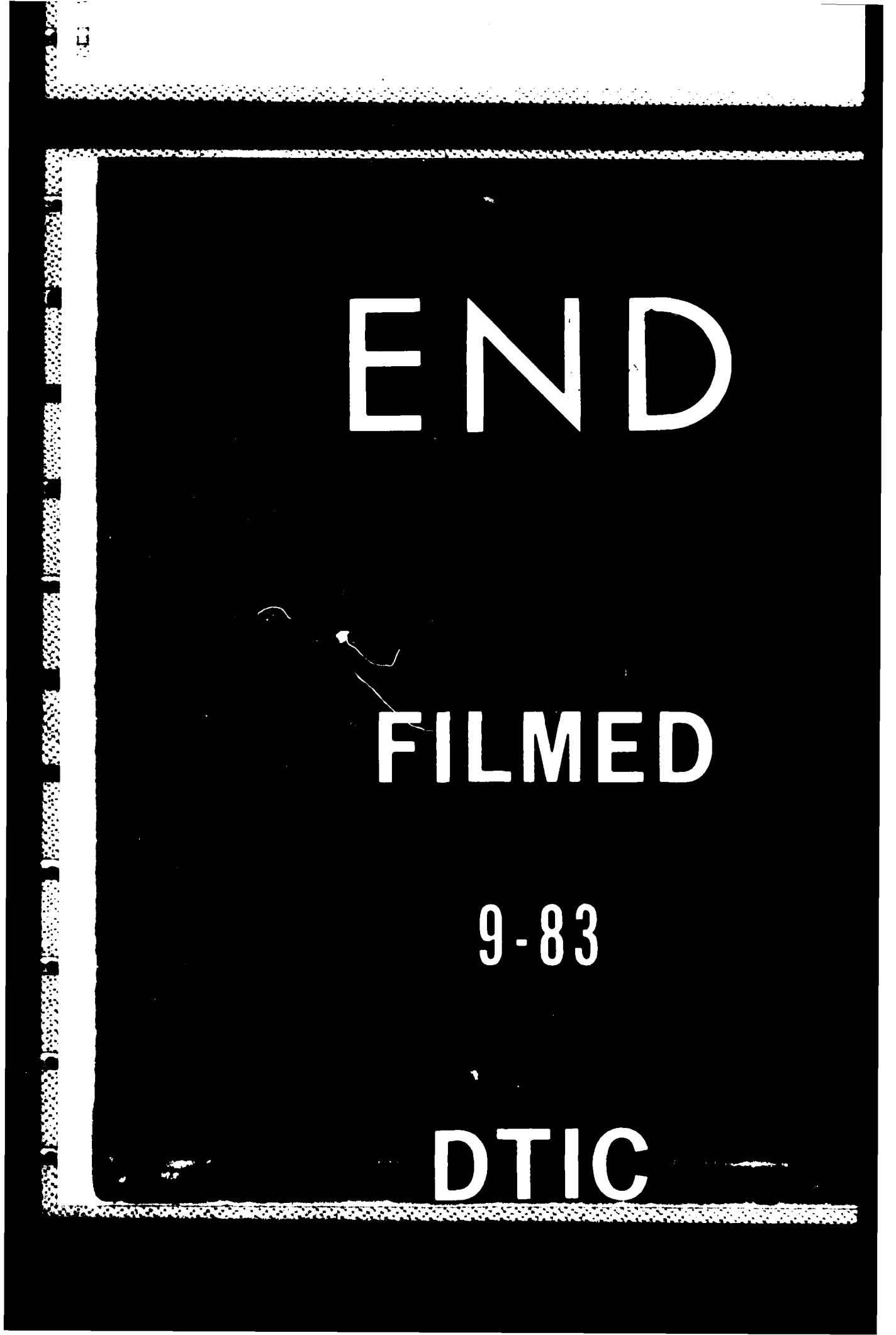
END
FILMED
9-83
DTIC